CHARACTERIZATION OF FATIGUE CRACK INITIATION CONDITION OF STEELS WITH AFM

Yoshikazu Nakai, Manabu Kishimoto, and Shohei Hosomi
Graduate School of Science and Technology, Kobe University, Nada, Kobe 657-8501, Japan

Abstract

Slip-band formation and fatigue crack-initiation processes in a high strength steel and a stainless steel were observed by means of atomic force microscopy (AFM). In the high strength steel, fatigue cracks were initiated in the slip band just adjacent to the inclusions. In the stainless steel, they were initiated in the slip bands near the grain boundaries. The slip distance could be evaluated from intrusion depth and slip band angle relative to the stress axis. In both materials, the distance increased linearly with the logarithm of the number of cycles. When the slip distance reached a critical value, a transgranular crack was initiated from the slip band, and the slope of the relationship was changed with crack initiation. For every crack initiation site, the slip distance at the crack initiation was almost identical, and this critical value was about 80 nm for the two steels. In α-brass, this critical value was 380 nm. Then this critical value may be controlled by atomic binding energy or atomic spacing independent of microstructure of the material.

1. INTRODUCTION

It is well known that the fatigue process of metallic materials without macroscopic defects can be divided into initiation and growth processes of cracks and final unstable fracture. Among these processes, various studies have been conducted on the crack-growth behavior, and that can be quantitatively analyzed based on the fracture mechanics [1]. The study on fatigue crack initiation is especially important for fatigue damage evaluation of micro-machine components because the fatigue life of these components is almost the crack initiation life [2]. The initiation condition of fatigue micro-cracks, however, still has not clarified enough, because no method for successive, direct and quantitative observation of the process had been devised.

For components without significant internal defects, the free surface is normally the site for the fatigue crack initiation, then the microscopic observation is the most useful method to clarify the mechanisms of the fatigue processes in materials, and the progress of metal fatigue study has strongly depended on the development of new microscopic observation methods. With conventional microscopes, such as optical microscopes, transmission electron microscopes (TEM), and scanning electron microscopes (SEM), however, successive, quantitative three-dimensional observations of the crack nucleation site in the specimen surface could not be conducted. Then, in most of these studies, the crack-initiation mechanisms were discussed qualitatively.

Since the surface morphology of materials can be observed with atomic-scale resolution, the scanning atomic force microscopy (AFM) is a powerful technique to study the mechanisms of fatigue and fracture of solid materials. Nakai and his co-workers studied fatigue slip-bands, fatigue crack-initiation, and the growth behavior of micro-cracks in a structural steel [3], and α-brass [4-11]. They reported for α-brass under cyclic bending that the depth of an intrusion increased with the number of stress cycles, and the depth drastically increased with crack initiation. The critical value for crack initiation was given as a function of the slip-band angle relative to the stress axis. From the AFM observations and geometrical consideration, it was found that the slip distance at the crack initiation was independent of the slip-band angle relative to the stress axis,

the stress amplitude, and the grain-size. They also reported that the critical value of the slip distance for cyclic torsion was identical for cyclic bending. In the present paper, the fatigue slip-band formation and the crack initiation processes in a high strength steel and an austenitic stainless steel were examined by means of AFM to elucidate fatigue crack initiation condition.

2. THEORY

Condition for the transgranular fatigue crack initiation can be analyzed by a geometrical model proposed by Tanaka and Nakai [12], which explains the relation between the surface-step and the slip direction. The surface-step, d, induced by a slip is

$$d = s \sin\beta \cos\alpha' \quad (1)$$

where the value of s is the slip distance in the slip-direction, the value of α' is the angle between the normal of the surface and the trace of the slip-band on the plane that is perpendicular to the surface and parallel to the loading-axis, and the value of β is the angle between the slip-direction and the slip-traces on the surface (see Fig. 1). Although fatigue slip bands are not steps like Fig. 1, but they are intrusion and intrusions, eq. (1) can be applied to fatigue slip bands because they are consequences of each step generated at each cycle.

The values of α' and β can be measured by the electron back scattering pattern (EBSP) method. For the case of face-centered cubic (FCC) crystals, slip occurs most often on {111} planes and in <110> directions. In all, there are 12 slip systems (four {111} planes and three <110> slip directions for each {111} plane). With the EBSP method, one of {111} planes and one of <110> slip direction can be identified. Other planes and directions can be determined from the geometrical relationships for FCC crystal. Since a slip line on surface is an intersection line of slip plane and surface plane, the actual slip plane can be identified from EBSP method and the actual slip line observed by microscopy. The value of β can be estimated by assuming that Schmid factor of the actual slip direction is larger than that of others.

For isotropic homogeneous material under uniaxial normal stress, lots of planes can be the maximum resolved shear stress plane whose normal has the angle of 45° from the loading axis as shown in Fig. 2 (a). Then, in polycrystalline materials, there are many grains whose slip plane is very close to the maximum resolved shear stress plane, and cracks are considered to be initiated from slip bands, which had slip systems in the maximum resolved shear stress direction [12]. For slip-bands, where the resolved shear stress along the slip-direction takes the maximum value, the following relationship should be satisfied.

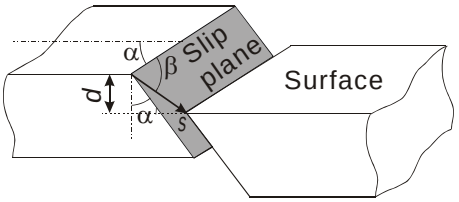

Fig. 1 Slip plane and slip direction.

$$\cos\beta = \cos\alpha \quad (2)$$

$$\cot^2\alpha + \tan^2\alpha' = 1 \quad (3)$$

where the value of α is the angle between the loading-axis and the trace of the slip-band on the surface. The value of slip distance can be calculated from the measured values of the depth of intrusion, d, and slip band angle, α, by substituting these values into eqs. (2), (3), and eq. (1).

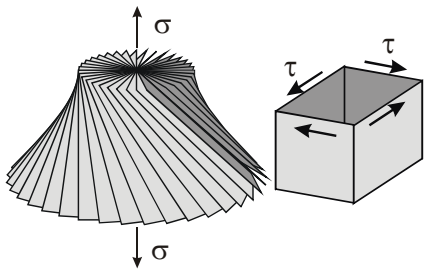

(a) Uniaxial tension stress (b) Shear stress

Fig. 2. Maximum shear stress planes.

The relation between the slip distance and the number of cycles in uniaxial loading (bending) fatigue

test of α-brass (R=0) is shown in Fig. 3, where open marks indicate data before the crack initiation, and solid marks show data after the crack initiation. The values of α are also indicated in the figure. The slope of the line is changed with crack initiation, and cracks are initiated from slip bands when the slip distance reached a critical value. This critical value is 380 nm independent of stress amplitude. The value was also found to be independent of stress ratio, grain size, and stress state (bending *vs.* torsion)[7-11].

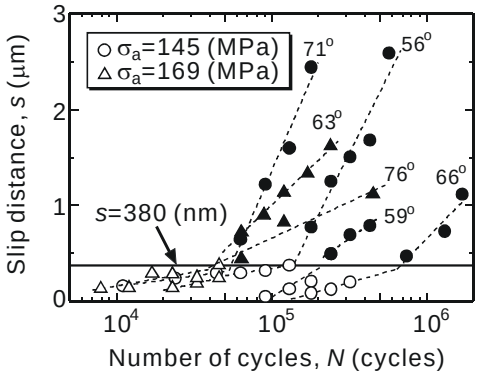

Fig. 3. Change of slip distance with stress cycles.

3. EXPERIMENTAL PROCEDURE

The materials for the present study were a high strength steel (0.2% proof strength: 463 MPa, Tensile strength: 653 MPa), and an austenitic stainless steel (Type 304, 0.2% proof strength: 280 MPa, Tensile strength: 572 MPa). Before fatigue tests, surface of the specimens were electro-chemically polished. As shown in Fig. 4, the specimen has a minimum cross-section of width 8 mm, and a thickness of 3 mm. The fatigue tests were carried out in a computer-controlled electro-dynamic vibrator operated at a frequency of 30 Hz under fully reversed cyclic plane bending moment (R = -1). To conduct a quantitative analysis of the development of fatigue slip-bands, the scanning atomic force microscopy (AFM) was employed for the present study. The scanning area for the observations was 20 μm×20 μm. Since it was very difficult to identify in advance where fatigue cracks would be initiated, replicas of the specimen surface were taken at the predetermined number of fatigue cycles. With resonance type testing machine, static loading was not easy, then the AFM images were taken at the unloading state. The replica films were coated by gold (Au) before observation. Although the height of the surface in the replica film was reversed from the specimen surface, the height of the replica film in the AFM images was reversed by an image processing technique.

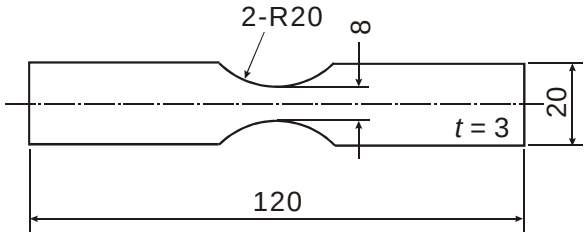

Fig. 4. Shape and dimensions of specimen (in mm).

4. EXPERIMENTAL RESULTS

4.1 High strength steel

In this material, many small pits were formed during surface polishing, and most of fatigue cracks were initiated from slip bands, which were formed adjacent to the pits. The pits are considered to be the traces of non-metallic inclusions. Figure 5 shows an example of optical micrograph of the crack initiation site, where the stress amplitude, σ_a, was 450 MPa.

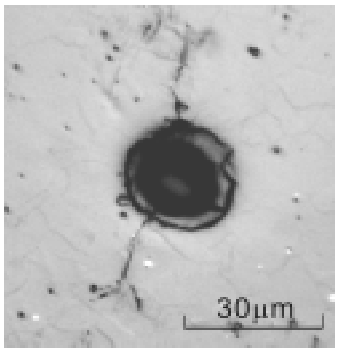

Fig. 5. Crack initiation site in high strength steel.

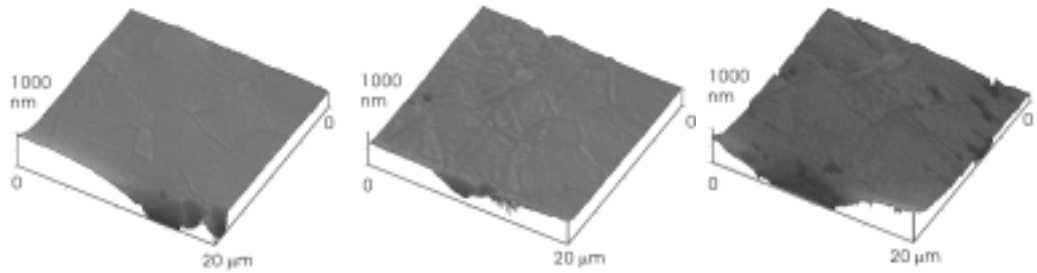

(a) 5.0x10^{3}cycles (b) 4.4 x 10^4 cycles (c) 4.6 x 10^4 cycles

Fig. 6 AFM images of crack initiation site in high strength steel.

AFM images of slip-bands formed at the crack initiation site are shown in Fig. 6. From the AFM images, the development of slip bands and initiation crack can be observed. For the quantitative analysis of slip band development, changes of the slip distance with the number of cycles is shown in Fig. 7, where the depth of slip band was measured at the deepest point of each slip band, and the slip distance was evaluated by eqs (1)-(3). The relationship can be expressed as bi-linear curve in semi-log plot, *i.e.*, the value of slip distance increases with the logarithm of the number of cycles, and the slope is changed with the crack initiation. The slip distance at the crack initiation is 80 nm, which value is different from that of α-brass.

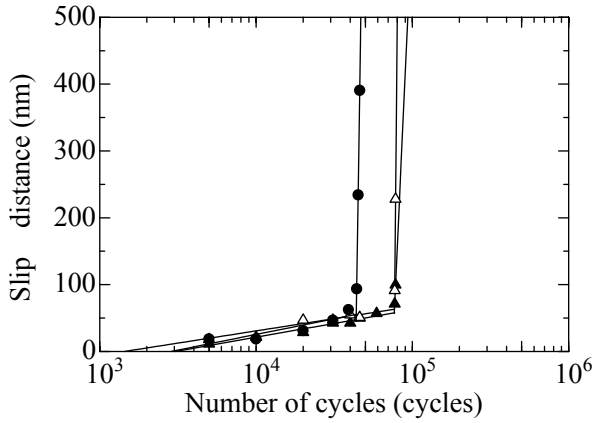

Fig. 7 Change of slip distance with number of cycles in high strength steel.

4.2 Stainless steel

An optical micrograph of the crack initiation site in this material is shown in Fig. 8, where the stress amplitude of the fatigue test was 375 MPa and the number of cycles to failure was 5.4x10^{4}cycles. AFM images, those are shown in Fig. 9, were obtained from the area which is surrounded by a rectangle shown in this micrograph. The crack initiation mechanism was almost the same as that for α-brass. Fatigue cracks were always initiated in slip bands near the grain boundary, which can be easily identified from the directions of slip bands, and the crack length just after the initiation was much shorter than the grain size.

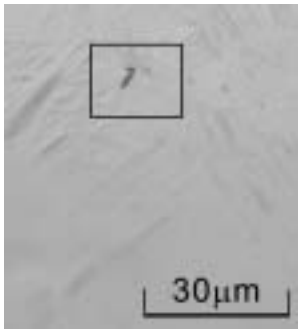

Fig. 8 Crack initiation site in stainless steel.

Changes of the slip distance with the number of cycles are shown in Fig. 10. The relationship for the main crack can also be expressed as bi-linear curve in semi-log plot, *i.e.*, the value of slip distance increases with the logarithm of the number of cycles, and the slope was changed with crack initiation. The slip distance at the crack initiation was 80 nm, which value is almost identical to

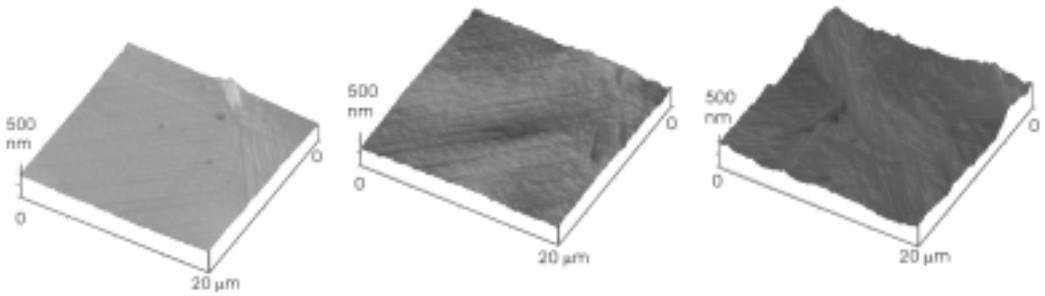

(a) 4.0×10^3 cycles (b) 1.5×10^4 cycles (c) 2.3×10^4 cycles

Fig. 9 AFM images of crack initiation site in stainless steel.

that for the high strength steel, and different from that of α-brass.

The relationships for other slip bands where cracks were not initiated until the end of the fatigue test (specimen failure) are also plotted in this figure. For these slip bands, the relationships were also linear, and the slip distances at the end of fatigue test were lower than that for the crack initiation (80 nm).

5. DISCUSSION

Three materials have been examined to elucidate transgranular fatigue crack initiation condition in slip band. In every material, the slip distance increased linearly with the logarithm of the number of cycles, and fatigue cracks were initiated when the slip distance reached to the critical value. The critical values for two steels are almost identical although their microstructure and strength are different. The critical value for α-brass value, however, was different from the value for steels. Therefore, the critical value may be is controlled by atomic binding energy, atomic spacing, Burger's vector of dislocations, etc.

Although the strengths of bulk material did not affect the critical value for the fatigue crack initiation, however, they affected the growth rate of slip distance, *i.e.*, the crack initiation life. The growth rate depended not only on bulk strength of material, but also on many factors. Even for the slip bands in the same specimen, the rate was not a unique value. It may be affected by many factors, for example, crystal orientation, grain size (or slip band length), and constraint of displacement by the adjacent grains, and then the crack initiation life was different in each grain. It is the reason why the predictions of crack initiation site and life have been very difficult task in fatigue studies. The observation of slip bands with AFM can enable the prediction because the slip distance increased linearly with the logarithm of the number of cycles, and the growth rate can be measured experimentally.

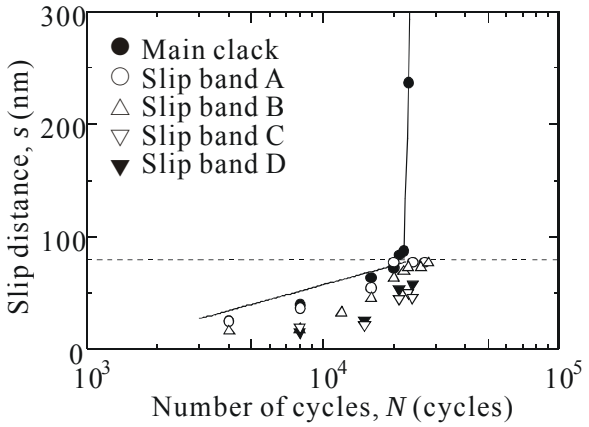

Fig. 10 Change of slip distance with number of cycles in stainless steel.

CONCLUSIONS

The fatigue slip-band formation and fatigue crack-initiation process in a high strength steel and an austenitic stainless steel were observed by means of scanning atomic force microscopy (AFM), and the following results were obtained.

(1) In the high strength steel, fatigue cracks were initiated in the slip band just adjacent to inclusions. In the stainless steel, they were initiated in slip band near the grain boundary.

(2) The slip distance could be evaluated from intrusion depth and slip band angle relative to the loading axis. In both materials, the distance increased linearly with the logarithm of the number of cycles. When the slip distance reaches a critical value, a transgranular crack was initiated from the slip band, and the slope of the relationship was changed with the crack initiation.

(3) For every crack initiation site, the slip distance at crack initiation was almost identical, and this critical value was about 80 nm for two kind of steel. In α-brass, this critical value was 380 nm. Then the critical value is controlled by atomic binding energy or atomic spacing independent of microstructure of the material.

ACKNOWLEDGMENT

Support of this work by Grant-in-Aid for Promotion of Steel Research by Iron and Steel Institute of Japan is gratefully acknowledged. The authors also express their applications to Kobe Steel Ltd. and Sumitomo Metal Industries, Ltd. for providing the material used in this study.

REFERENCES

1. Tanaka, K.,echanisms and mechanics of short fatigue crack propagation, JSME Int. J., **30**, pp.1-13 (1987).
2. Nakai, Y., Hiwa, C., Imanishi, T., and Hashimoto, A., Size Effect on Fatigue Strength of Metallic Micro-materials Proceedings of Asian-Pacific Conference on Fracture and Strength '99, SM22 (1999).
3. Nakai, Y., Fukuhara, S., and Ohnishi, K., Observation of fatigue damage in structural steel by scanning atomic-force microscopy, International Journal of Fatigue Int. J. Fatigue, **19**, pp.S223-S236 (1997).
5. Nakai, Y., Ohnishi, K., and Kusukawa, Observation of fatigue crack initiation process in α-brass by AFM, T., Trans. JSME, **65A**, pp.483-490 (1999).
6. Nakai, Y., Ohnishi, K., and Kusukawa, T., Observations of Fatigue Slip Bands and Stage I Crack Initiation Process in α-brass by Scanning Atomic-force Microscopy, Small Fatigue Cracks: Mechanics and Mechanisms, Elsevier, pp.343-352 (1999).
7. Nakai, Y., Kusukawa, T., and Hayashi, N., Grain-Size Effect on Fatigue Crack Initiation Condition Observed by Using Atomic-Force Microscopy, ASTM STP 1406, pp.122-135 (2001).
8. Nakai, Y. and Kusukawa, Quantitative evaluation of sli-band growth and crack initiation in fatigue of 70-30 brass by means of atomic-force microscopy, T., Trans. JSME, **67A**, pp.476-482 (2001).
9. Nakai, Y. and Maeda, K., Prediction of Crack Initiation under Cyclic Normal and Shear Stresses by Means of Atomic-Force Microscopy, Fatigue 2002, pp.339-346 (2002).
10. Nakai, Y. and Maeda, K., Characterization of Fatigue Crack Initiation in α-Brass by Means of AFM and EBSP, Proceedings of ATEM'03, CD-ROM (2003).
11. Nakai, Y., Maeda, K., Observations of fatigue slip-band growth and crack initiation in α-brass under cyclic shear stresses by means of atomic-force microscopy, J. Soc. Mat. Sci., Jpn, **52**, pp.625-630 (2003).
12. Tanaka, K., Hojo, M., and Nakai, Y., Fatigue crack initiation and early propagation in 3% silicon iron, ASTM STP 811, pp.207-232 (1983).